Cancer Cell, Volume *14*

Supplemental Data

Article

Distinct Thresholds Govern

Myc's Biological Output In Vivo

Daniel J. Murphy, Melissa R. Junttila, Laurent Pouyet, Anthony Karnezis, Ksenya Shchors, Duyen A. Bui, Lamorna Brown-Swigart, Leisa Johnson, and Gerard I. Evan

Supplemental Experimental Procedures

Genotyping

The following primer sets were used for genotyping: *Rosa26* i) R26F2 – 5'AAA GTC GCT CTG AGT TGT TAT ii) R1295 – 5'GCG AAG AGT TTG TCC TCA ACC iii) R523 – 5'GGA GCG GGA ATG GAT ATG; *MycER* (MycERt) – 5'CCA AAG GTT GGC AGC CCT CAT GTC (MycS3) – 5'AGG GTC AAG TTG GAC AGT GTC AGA GTC.

Expression Analysis

Real time quantitative PCR (qPCR) was performed by the UCSF Comprehensive Cancer Center Genome Analysis core facility. The following primer/probe sets were used to detect the indicated mRNA transcripts: $MycER^{T2}$ (F) 5'ATT TCT GAA GAC TTG TTG CGG AAA (R) 5'GCT GTT CTT AGA GCG TTT GAT CAT GA (Probe) 5'FAM-CAT GTC TCC AGC AGA CCC CGG ATC CCG TAG CTG TTC AA-36TAMSp; mouse *c-Myc*: (F) 5'CGC GTC CGA GTG CAT TGA (R) 5'AGC AGC GAG TCC GAG GAA (Probe) 5'FAM-CGC CCA AAT CCT GTA CCT CGT CCG ATT CCA CGG CCT TCT-36TAMSp; human *c-Myc* (used to compare $MycER^{T2}$ with $MycER^{TAM}$): (F) 5'GCC CCT GGT GCT CCA TGA (R) 5'CAA CAT CGA TTT CTT CCT CAT CTT CT (Probe) 5'FAM-CAC CGC CCA CCA CCA GCA GCG AC-BHQ2; $p19^{ARF}$: (F) 5'AGA GGA TCT TGA GAA GAG GGC C (R) 5'GCA GTTCGA ATC TGC ACC (Probe) 5'FAM-AAT CCT GGA CCA GGT GAT GAT GAT GGG-36TAMSp; mouse *p21*: Mm00432448_m1 (Applied Biosystems) and mouse *PUMA*: Mm00519268_m1 (Applied Biosystems) as previously reported (Martins *et al.*, 2006).

Cell Culture and Immunoblotting

Embryonic fibroblasts were prepared from E13.5 *R26-lsl-*$MycER^{T2}$ and *R26-*$MycER^{T2}$ mice by standard technique. Whole cell lysates were prepared by dissolving cells in Tween lysis buffer [150 mM NaCl; 50 mM HEPES, pH 7.5; 1 mM EDTA; 2.5 mM EGTA; 0.1% Tween 20 + Complete protease inhibitor cocktail (PIs; Roche)] followed by sonication. Nuclear extracts were made in low salt buffer [20 mM KCl; 10 mM HEPES, pH 7.5; 1mM $MgCl_2$; 1 mM $CaCl_2$; 0.1% Triton x-100 + PIs]. For liver extracts, freshly isolated livers were homogenized in 10 vol/WT T-

Per (Pierce) + PIs, fractionated by centrifugation at 1,000 x G and the pellets re-suspended in 1 volume T-Per + 0.2% SDS, followed by sonication. Islets were prepared from disaggregated pancreata as previously described (Lawlor *et al.*, 2006) and lysed in Tween lysis buffer, sonicated and cleared by centrifugation at 12,000 x G prior to loading. For $p19^{ARF}$ analysis, cell lysates were loaded on glycerol/acrylamide gels and fractionated by discontinuous electrophoresis and electroblotted onto PVDF membranes. Anti-ERα (Santa Cruz, SC-543); anti-c-Myc (Santa Cruz, SC42 and 9E10); X-Myc1 (G.I.E.); anti-$p19^{ARF}$ 5-C3-1 (Bertwistle et al., 2004), generously provided by Dr Martine Roussel, St Jude Hospital); anti-lamin A/C (Santa Cruz, SC7293); anti-β-actin (Sigma) were used as primary antibodies. Secondary antibodies were horseradish peroxidase-conjugated (Amersham) and were detected by chemiluminescence.

Immunohistochemistry and Immunofluorescence

Tissues were processed and sectioned by the UCSF Comprehensive Cancer Center Mouse Pathology core facility. 5 µm paraffin embedded sections were probed with Ki67 antibody (SP6, Neomarkers: Fremont, CA) was used at 1:200 in 3% BSA overnight (o/n) at $4^{\circ}C$ and detected with biotinylated goat anti-rabbit (Vector Labs) followed by Vectastain ABC detection (Vector Labs) using stable diaminobenzidine (DAB) solution (Invitrogen). For BrdU/IdU double staining, mouse a-BrdU (1:20, Roche), which recognizes both BrdU and IdU, was used in conjunction with rat a-BrdU (1:200, Serotec) that recognizes BrdU only. Bound primary antibodies were detected using Alexa-488 conjugated a-mouse IgG and Alexa-568 conjugated a-rat IgG (Molecular Probes). For $p19^{ARF}$ immunohistochemistry, blocking was performed in 10% normal goat serum (NGS) with 0.1% Triton x-100. Primary antibody (5-C3-1) was diluted 1:10 in 3% NGS + 0.1% Triton x-100 and incubated overnight at $4^{0}C$. TUNEL staining was performed using the ApopTag peroxidase labeled kit (Chemicon) or ApopTag fluorescein labeled kit (Chemicon) according to the manufacturers directions. Otherwise, tissue sections were blocked overnight in 3% BSA prior to addition of peroxidase-conjugated anti-digoxigenin.

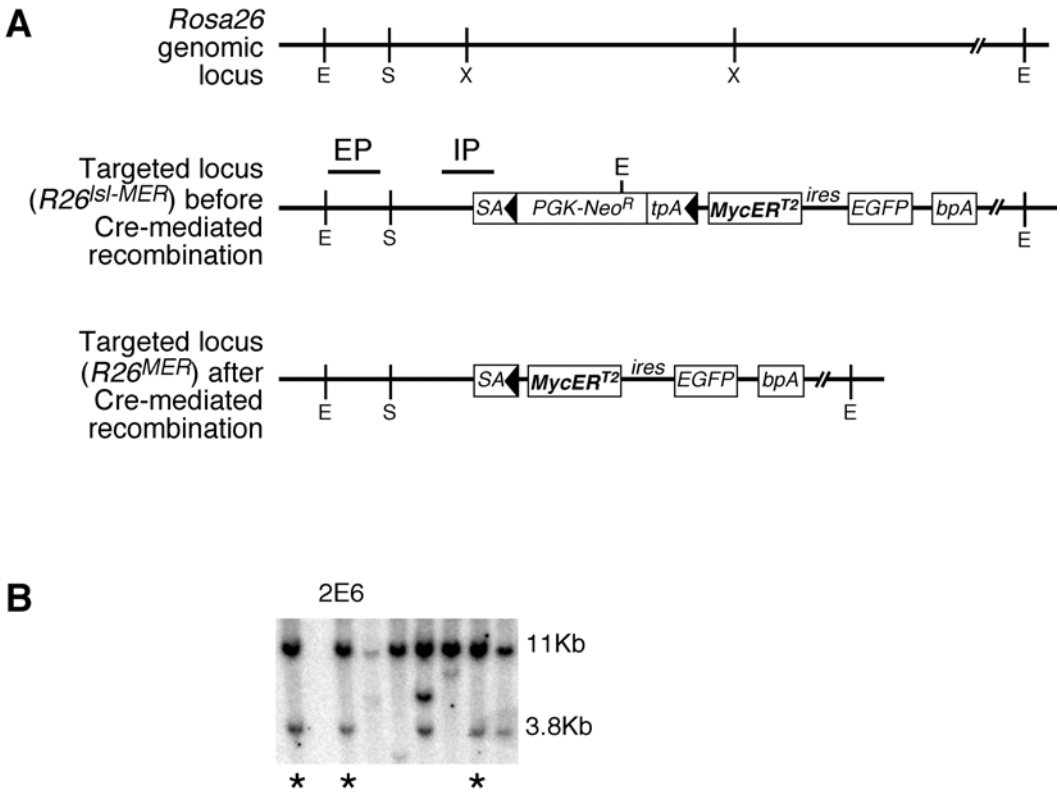

Figure S1. Targeted Insertion of Conditional *MycER^{T2}* cDNA into the *Rosa26* Locus

(A) Diagram of the *Rosa26* locus prior to and after insertion of the *lox-STOP-lox-MycER^{T2}* cassette and after Cre-induced excision of the floxed stop element. *SA* = splice acceptor sequence; *tpA* = triple repeat polyadenylation sequence; black arrowheads = *LoxP* sites; X = *XbaI*; E = *EcoRV*; S = *SacII*; *bpA* = *bovine papillomavirus polyadenylation signal*; EP = external probe; IP = internal probe. Adapted from Srinivas, *et al*. (1999).

(B) Southern blot of EcoRV digested genomic DNA from neomycin resistant ES cell clones with internal probe. The 11Kb band represents the endogenous *Rosa26* locus while the 3.8Kb band represents homologous recombination with the targeting vector. Lanes marked with an asterisk indicate detection of the appropriate bands with both internal and external probes. The *2E6* line yielded germ line transmission of the recombined allele.

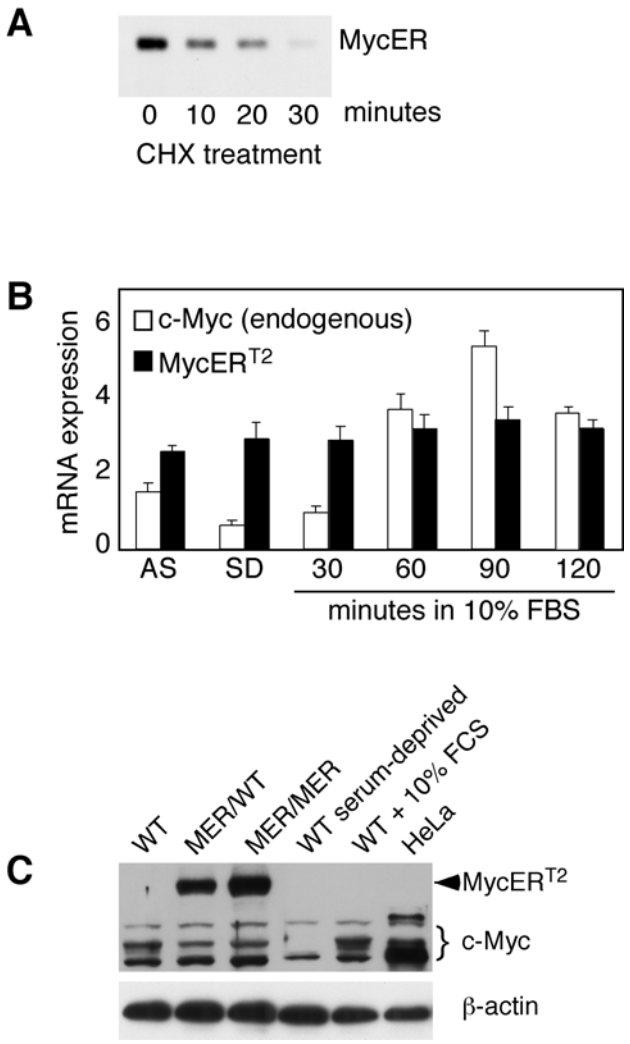

Figure S2. Comparison of Endogenous Myc and *R26*-Driven MycER^{T2} in MEFs

(A) MycER^{T2} has a very short half-life. Cyclohexamide (10 mg/ml) was added to log-phase *R26*$^{MER/WT}$ MEFs in full growth media for 0, 10, 20 and 30 minutes prior to lysis. MycER^{T2} levels were then assayed by anti-ERα immunoblot.

(B) Endogenous Myc is regulated by serum but *R26*-driven MycER^{T2} is not. Real-time quantitative PCR (qPCR) comparison of *MycER*^{T2} and endogenous c-*myc* in *R26*$^{MER/WT}$ MEFs under conditions of serum deprivation followed by acute serum re-stimulation for the indicated durations (n = 3). AS = asynchronously proliferating cells in growth media; SD = serum-deprived cells (0.2% FBS overnight). mRNA levels are normalized to *L19*.

(C) Activation of MycER^{T2} does not significantly autosuppress expression of endogenous Myc in *R26*$^{MER/WT}$ or *R26*$^{MER/MER}$ MEFs. Cell lysates derived from WT, *R26*$^{MER/WT}$ and *R26*$^{MER/MER}$ MEFs grown in complete medium + 100 nM 4-OHT to activate MycER^{T2} were probed with anti-Myc antibody exactly as in Figure 1B.

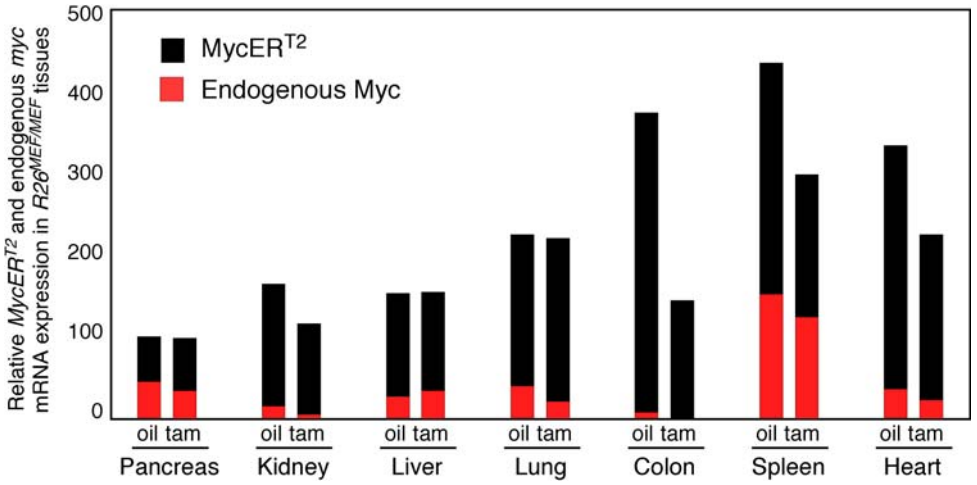

Figure S3. Direct Comparisons of Endogenous and MycER^{T2} mRNA Levels in Various Tissues of Adult Homozygous *R26*$^{MER/MER}$ Mice

RNA was extracted from various tissues of adult homozygous *R26*$^{MER/MER}$ and relative expression levels of endogenous c-Myc and MycER^{T2} mRNA levels, as assayed by qPCR, are shown relative to *GUS*.

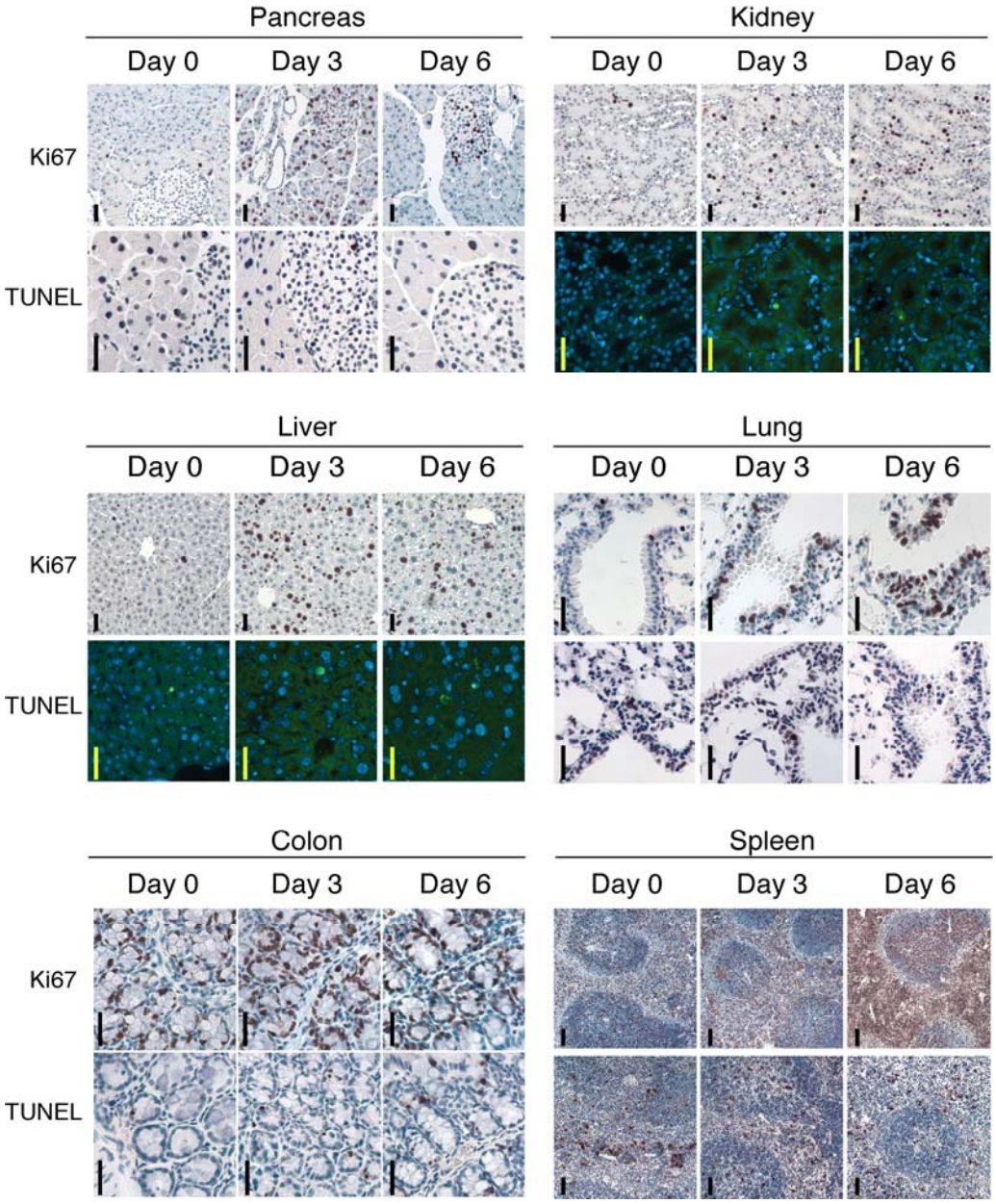

Figure S4. Myc Induces Proliferation without Apoptosis in Multiple Organs of *R26*$^{MER/MER}$ Mice

Ki67 and TUNEL staining of sections from organs of *R26*$^{MER/MER}$ mice treated for 0, 3 or 6 days with tamoxifen to activate MycER^{T2}. Scale bar = 50 mM.

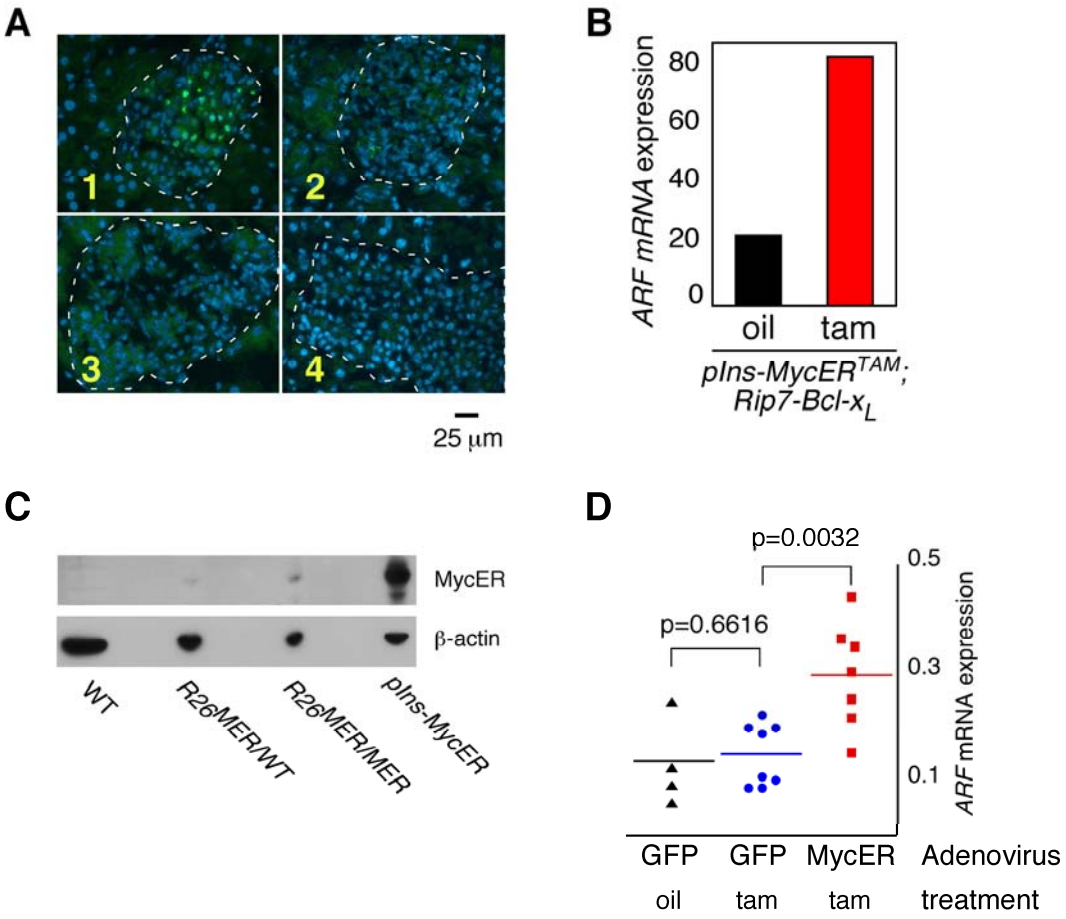

Figure S5. Low Levels of Deregulated Myc Fail to Engage the p19^{ARF}/p53 Pathway In Vivo

(A) Immunohistochemical analysis of p19^{ARF} protein induction following Myc activation in vivo in pancreatic islets of *pIns-MycER*^{TAM};*ARF*$^{+/+}$ (1), *pIns-MycER*^{TAM};*ARF*$^{-/-}$ (3), and *R26*$^{MER/MER}$ mice treated for 1 day with tamoxifen (2), and in *R26*$^{MER/MER}$ mice treated systemically for 3 days with tamoxifen (4). Specific nucleolar p19^{ARF} staining is observed only in tamoxifen-treated *pIns-MycER*^{TAM} islets, in which MycER^{TAM} expression is high (see also Figure S6).

(B) Induction of *ARF* mRNA by high levels of Myc in pancreatic β cells. qPCR analysis of *ARF* mRNA expression in pooled islets purified from pancreata of *pIns-MycER*^{TAM};*Rip7-Bcl-x*$_L$ mice treated for 3 days with oil carrier (n = 2) or tamoxifen (n = 2) was quantified by qPCR and normalized to *GUS*.

(C) Anti-c-Myc immunoblot of fractionated pancreatic islet lysates derived from WT and *R26MER* mice (all tamoxifen-untreated).

(D) Elevated levels of Myc induce *ARF* expression in lung. *R26*$^{lsl\text{-}MER/lsl\text{-}MER}$ mice were infected by inhalation with recombinant adenoviruses expressing either Cre recombinase or MycER$^{T2.}$ Mice were then treated for 3 days with either oil or tamoxifen to activate MycER^{T2}, lung tissue isolated by laser capture microdissection and relative ARF *mRNA* levels quantitated by qPCR. Each point represents assay data from a single mouse.

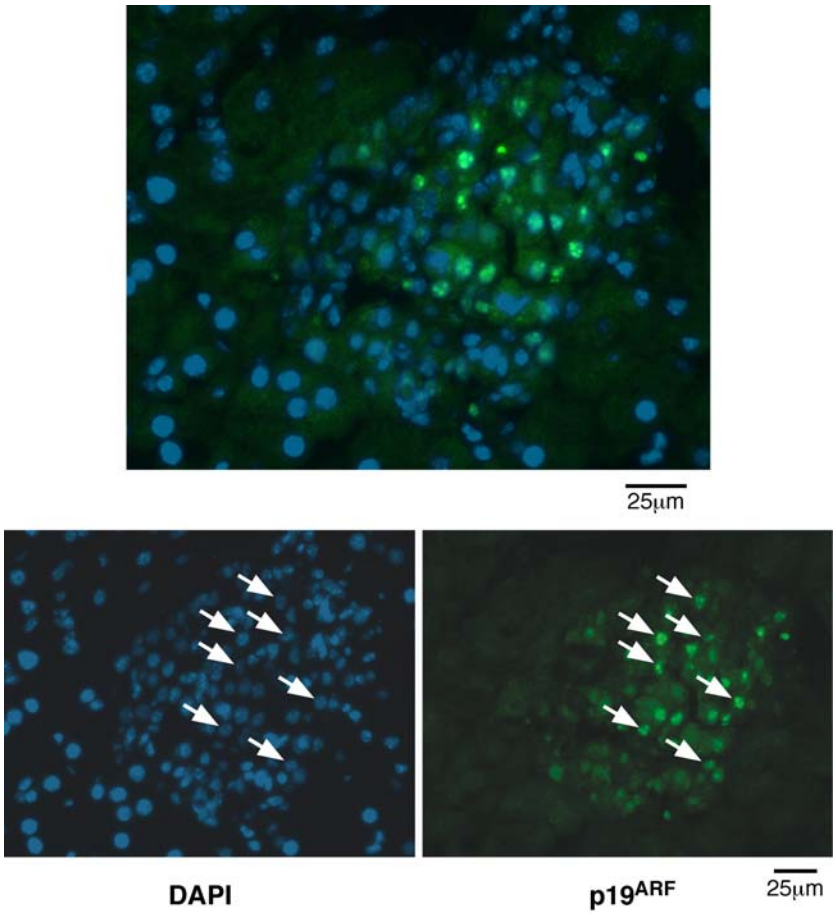

Figure S6. High-Power p19^{ARF} Immunohistochemistry of Islet Sections from *pIns-MycER*^{TAM} Mice in Figure S5A, Showing Localization of p19^{ARF} to Nucleoli of β Cells

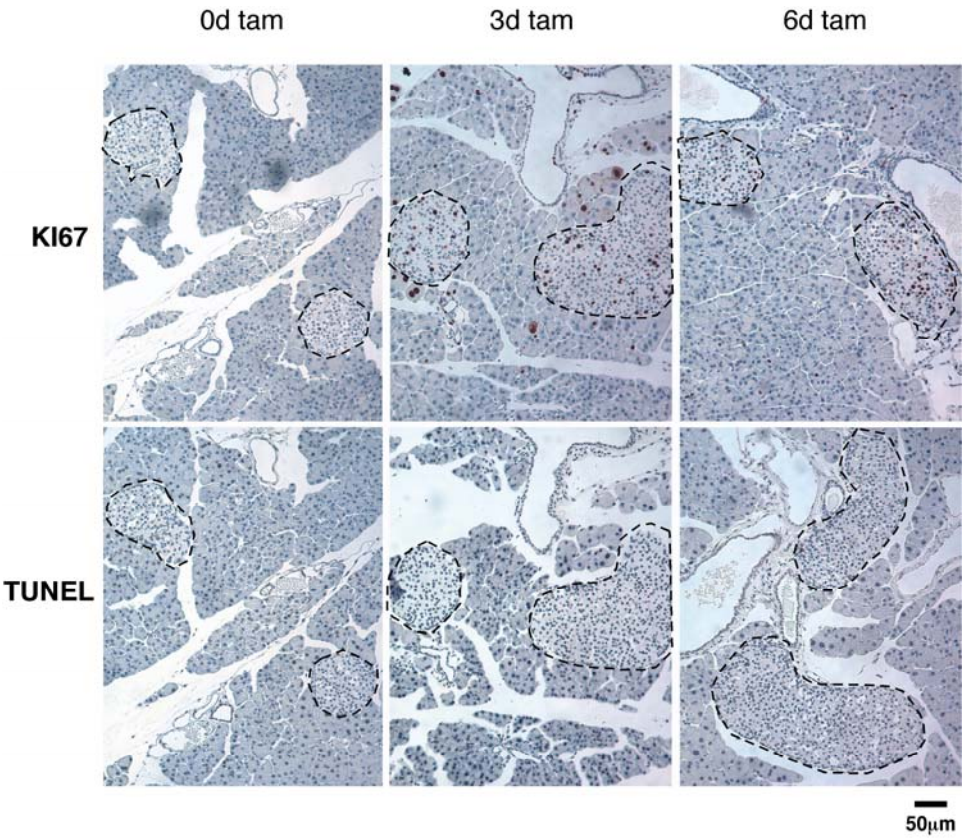

Figure S7. Induction of Apoptosis Requires Higher Levels of Deregulated Myc than Induction of Ectopic Proliferation

Lower-magnification images of sections of pancreatic islets from *R26*$^{MER/MER}$ mice, per Figure 5B.

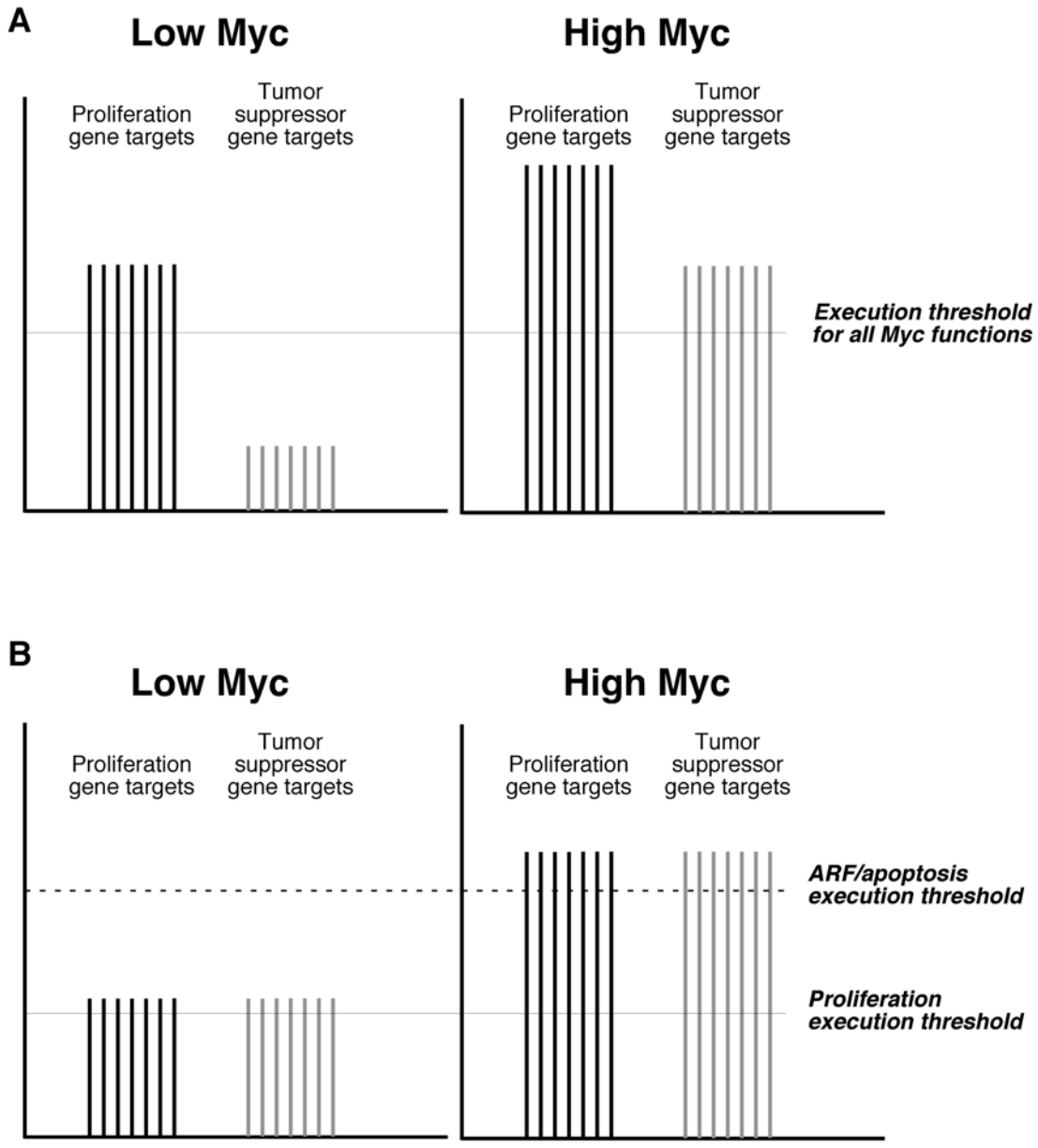

Figure S8. Models for How Differing Myc Threshold Levels Determine the Distinct Biological Outputs of Proliferation versus Apoptosis

(A) Low and high levels of Myc engage distinct gene sets that are, respectively, proproliferative and proapoptotic (i.e. Myc discriminates).

(B) Conversely, high and low levels of Myc regulate the same genes but to an overall greater extent when Myc is high: in this case, the different biological outcomes of proliferation versus apoptosis are not due to the outputs of differing gene sets but to different thresholds at which the proliferative and apoptotic gene programs engage their effector pathways (i.e. downstream factors decide).

Table S1. Proliferation and Apoptosis Induced by Acute MycER^{T2} Activation in *R26*$^{MER/WT}$ and *R26*$^{MER/MER}$ Mice

		R26$^{MER/WT}$ Myc Induced		*R26*$^{MER/MER}$ Myc Induced	
Organ	Tissue	Proliferation	Apoptosis	Proliferation	Apoptosis
Pancreas	Endocrine	No	No	Yes	No
	Exocrine	No	No	Yes	No
Kidney	Cortex	No	No	Yes	No
	Medulla	No	No	No	No
Liver	Mature Hepatocytes	No	No	Yes	No
	Other Cell Types	No	No	Yes	No
Lung	Bronchiolar Epithelium	No	No	Yes	No
Intestine	Small*	Not Evdnt	No	Not Evdnt	Yes
	Large	Yes	No	Yes	Yes
Spleen	Red Pulp*	Yes	Not Evdnt	Yes	Not Evdnt
	White Pulp*	Not Evdnt	Not Evdnt	Yes	Not Evdnt
Thymus	Cortex*	Not Evdnt	Not Evdnt	Not Evdnt	Not Evdnt
	Medulla*	Not Evdnt	Not Evdnt	Not Evdnt	Not Evdnt
Skin	Epidermis	No	No	Yes	No
	Dermis	No	No	Yes	No
Muscle	Skeletal	No	No	No	No
	Cardiac	No	No	No	No
Brain	Neuronal	No	No	No	No
	Glial	No	No	No	No
	Epithelial	No	No	Yes	No

* The high rate of intrinsic proliferation and/or apoptosis in these tissues may obscure the immediate consequences of acute Myc deregulation

Extent of cell proliferation was determined immunohistochemically in tissue sections by staining for Ki67 and/or BrdU/IdU incorporation. Apoptosis was analyzed in tissue sections by TUNEL staining.